Research Article

Journal of Environmental Nanotechnology

Plant-derived *Bixa orellana* (Annatto)-based Histochemical Staining Incorporating Iron Oxide Nanoparticles: A Pilot Study of Oral Tissue Staining and Potential Environmental Relevance

Akshara Modak[1], R. Abilasha[1*], Anoop Kumar[1] and Saheb Ali[2]

[1]Department of Oral Pathology and Microbiology, Saveetha Dental College and Hospitals, Saveetha Institute of Medical and Technical Sciences, Saveetha University, Chennai, TN, India

[2]Department of Periodontics, Saveetha Dental College and Hospitals, Saveetha Institute of Medical and Technical Sciences, Saveetha University, Chennai, TN, India

Received: 07.07.2026 Accepted: 10.08.2026 Published: xx.xx.xxxx

*abilasha.ramasubramanian@gmail.com

ABSTRACT

Conventional histological staining workflows involve multiple chemical reagents, creating interest in plant-derived staining components as potential alternatives for more environmentally responsible laboratory practices. This pilot study evaluated the histochemical staining characteristics of fresh annatto, commercial annatto, and an iron oxide nanoparticle-incorporated annatto formulation in selected oral tissues, with hematoxylin and eosin (H&E) and conventional special stains serving as reference methods. The primary objective was to compare tissue-staining patterns, descriptive staining scores, and staining distributions across collagen-rich, keratinized, odontogenic, vascular, ductal, and adipose components. Natural and commercial annatto were assessed at 5, 15, and 30 min, with 5 min selected for subsequent comparison based on preliminary qualitative visual assessment. The nanoparticle-incorporated formulation was characterized using Fourier-transform infrared spectroscopy (FTIR) and X-ray diffraction (XRD). FTIR showed bands at 3261.3, 2931.8, 1605, 1399.4, 1042.8, 885.24, 715.04, and 586.5 cm^{-1}. XRD showed diffraction features at 2θ values ranging from 16.933° to 78.218°, with reported crystallite-size estimates of 17.4–69.6 nm; these values were not interpreted as particle sizes. Annatto showed staining affinity mainly for collagen-rich connective tissue, with additional staining of keratinized, vascular, ductal, and adipose components. The overall descriptive scores were 63.85% for natural annatto, 66.50% for commercial annatto, 71.10% for the nanoparticle-incorporated formulation, 74.17% for conventional special stains, and 84.73% for H&E. The findings indicate preliminary histochemical staining affinity of annatto, but they do not establish diagnostic specificity, equivalence to conventional stains, or its suitability as a diagnostic replacement. Further studies with complete specimen-level data, standardized staining protocols, direct nanomaterial characterization, and inferential analysis are required to evaluate the reproducibility, performance, and potential environmental benefits of annatto-based staining components.

Keywords: Bixa orellana (annatto); Histochemical staining; Iron oxide nanoparticles; Environmental relevance.

1. INTRODUCTION

Histological staining is fundamental to oral pathology because it permits assessment of tissue architecture and selected cellular or extracellular components. H&E provides routine morphological contrast, whereas special stains such as Masson's Trichrome, Van Gieson, and Ayoub–Shklar are used when additional contrast for collagen-rich or keratinized structures is required. Their established diagnostic roles provide appropriate reference standards against which experimental staining agents can be evaluated.

Conventional histology workflows may require multiple dyes, acids, alcohols, and organic solvents. Xylene is widely used for tissue clearing and deparaffinization and is recognized by the National Institute for Occupational Safety and Health as an occupational chemical hazard; laboratory workers can be exposed during histologic processing (NIOSH 2019). This has encouraged investigation of alternative staining components; however, a plant-derived reagent should not be assumed to be safer or more sustainable without direct assessment of its composition, solvent use, waste, toxicity, and performance.

Bixa orellana L. (annatto) is a plant-derived colorant whose seeds contain the carotenoid pigments bixin and norbixin. These chromophoric compounds provide the characteristic yellow-orange to red coloration and are relevant to staining because pigment extraction and dispersion influence the visible contrast produced in tissue sections (Shahid-ul-Islam et al. 2016). Experimental studies have investigated annatto-derived preparations as natural histological stains, but staining

performance varies with tissue type and preparation, and evidence for oral histochemical applications remains limited (Aiswarya et al. 2025; Krampah et al. 2021).

Despite the use of annatto as a natural colorant and its investigation in histological staining, comparative evidence in oral tissues encompassing collagen-rich lesions, keratinized structures, odontogenic tissues, and ductal or vascular components remains limited. Natural extracts may also show variable pigment distribution and staining intensity. The present study therefore incorporated iron oxide nanoparticles into the annatto preparation as an experimental formulation intended to modify pigment dispersion and tissue–stain interaction. This rationale is exploratory, as the study did not directly measure nanoparticle-mediated dispersion, tissue binding, or the mechanism responsible for any difference in staining.

Annatto-based nanostructures have been explored in biomedical applications, and nanomaterial-assisted formulations may modify the distribution or surface interaction of plant-derived compounds; however, such effects require direct experimental demonstration in the specific formulation being studied (Silva et al. 2024). The present formulation was characterized using FTIR and XRD, but direct particle morphology, particle-size distribution, DLS, PDI, zeta potential, and formal stability testing were not available. These characterization limitations are addressed later in the manuscript in the Discussion section and are not used to define the formulation as a nanoemulsion.

The primary aim of this pilot study was to compare the descriptive histochemical staining characteristics of fresh annatto, commercial annatto, and an iron oxide nanoparticle-incorporated annatto formulation with H&E and selected conventional special stains in oral tissues. A secondary aim was to cautiously describe the potential environmental relevance of an annatto-based staining component, without making quantitative sustainability claims that were not directly assessed.

2. MATERIALS AND METHODS

2.1 Study Design and Tissue Selection

This pilot comparative histochemical study evaluated fresh, commercial, and iron oxide nanoparticle-incorporated Bixa orellana (annatto) preparations as experimental staining agents in selected oral tissue specimens. Formalin-fixed, paraffin-embedded specimens represented fibroma, oral submucous fibrosis (OSMF), well-differentiated oral squamous cell carcinoma (OSCC), odontoma, ameloblastoma, ductal papilloma, and lymph node tissue. These categories represented collagen-rich connective tissue, keratinized epithelium, odontogenic/mineralized components, ductal structures, adipose tissue, and vascular structures. Serial sections, approximately 4–5 µm thick, were prepared from the selected paraffin blocks. The study records did not document the exact number of specimens, blocks, or sections evaluated for each category, nor did it retain a detailed sampling procedure; these items therefore cannot be reconstructed retrospectively.

2.2 Ethical Approval

The study was reviewed and approved by the Institutional Human Ethical Committee (IHEC) of Saveetha Dental College and Hospitals, Saveetha Institute of Medical and Technical Sciences, Chennai, Tamil Nadu, India, under approval number IHEC/SDC/OPATH-2303/26/107. The study was conducted in accordance with the ethical requirements specified by the institutional committee and the terms of the granted approval.

2.3 Preparation of Annatto Extracts

Natural annatto extract was prepared from 0.5–1 g of Bixa orellana seeds. The seeds were finely ground and extracted with 10–20 mL of distilled water or 30% ethanol, then heated at 70–80 °C for 30 min with occasional stirring and filtered through Whatman No. 1 filter paper. The study records did not identify the solvent used, the exact sample-to-solvent ratio, the exact extraction temperature within the reported range, the extraction yield, or the final extract concentration. These parameters were therefore not inferred. A commercially available annatto preparation was used directly. Natural and commercial preparations were evaluated at 5, 15, and 30 min during preliminary optimization, after which 5 min was selected on the basis of qualitative visual observations.

Article in Press

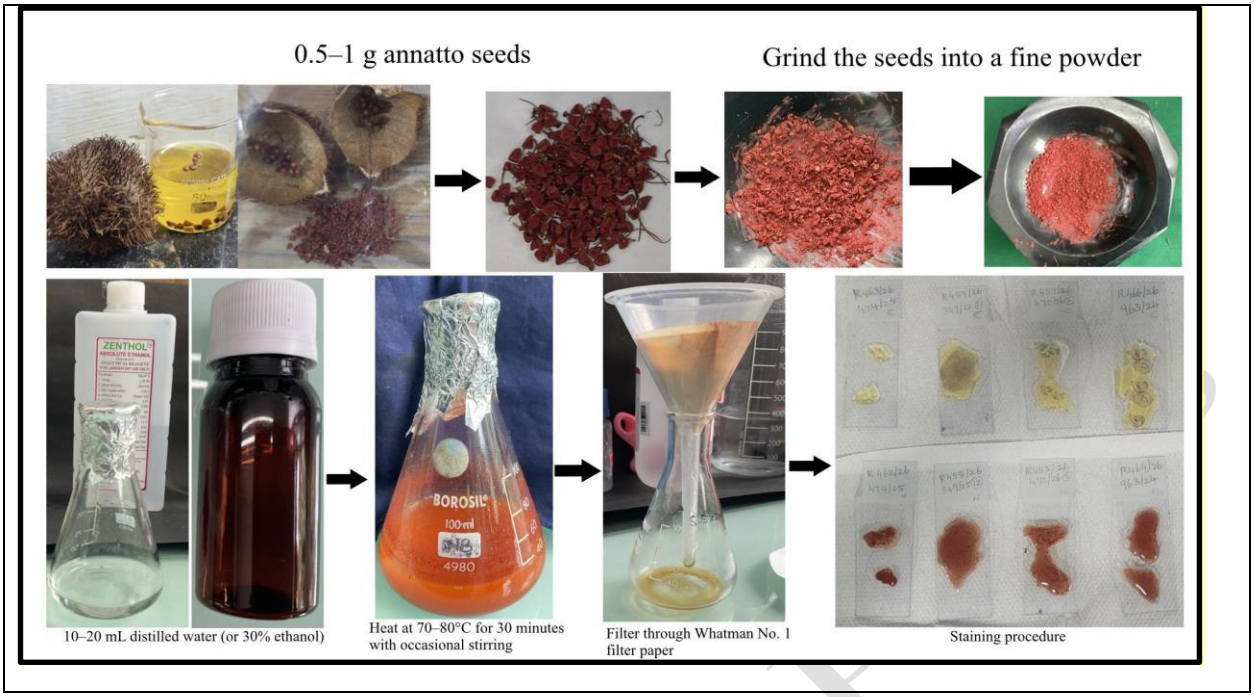


Fig. 1: Preparation of annatto stain for histopathology

2.4 Preparation of Iron Oxide Nanoparticle-Incorporated Annatto Formulation

Iron oxide nanoparticles (FeONPs) were reported to have been synthesized using 1 M ferric nitrate as the precursor. The study records did not contain the reaction temperature, reaction time, pH, reaction volume, precipitating or reducing agent, synthesis mechanism, drying temperature, nanoparticle identity, or exact quantity/concentration of FeONPs incorporated into the annatto extract. The nanoparticles were washed with distilled water and dried, after which a predetermined quantity was dispersed in crude annatto extract under continuous stirring. Because the missing synthesis and formulation parameters cannot be reliably reconstructed, the material is referred to as an iron oxide nanoparticle-incorporated annatto formulation rather than a chemically defined iron oxide phase or a fully characterized nanoemulsion.

2.5 Characterization of the Iron Oxide Nanoparticle-incorporated Annatto Formulation

The formulation was characterized using FTIR and XRD. FTIR was used to describe functional-group absorption bands and the spectral profile of the combined annatto–iron oxide preparation. XRD was used to describe diffraction features and estimate crystallite size. The study records did not retain the FTIR spectral range, resolution, or number of scans, or the XRD operating voltage, current, radiation source, scan range, step size, or scan rate. The calculation method and software used for the reported crystallite-size estimates and crystalline/amorphous fractions were also not documented. Accordingly, the XRD-derived 17.4–69.6 nm values are reported only as crystallite-size estimates and are not equated with particle size. No validated JCPDS/ICDD phase match was available, so a definitive Fe_3O_4, γ-Fe_2O_3, or α-Fe_2O_3 assignment is not made. Direct SEM/TEM, DLS, PDI, zeta potential, and formal stability testing were not performed or were not available in the study records.

2.6 Histopathological Staining

Histopathological staining was performed using natural annatto extract, commercial annatto, and the iron oxide nanoparticle-incorporated annatto formulation. Following deparaffinization in xylene, sections were rehydrated through descending grades of alcohol and stained with Harris hematoxylin for approximately 7 min, followed by bluing under running tap water. The respective annatto preparation was then applied as the experimental counterstain for 5 min to assess its ability to provide additional tissue contrast. Sections were washed with distilled water, cleared in xylene, and mounted with DPX. H&E and corresponding conventional special-stained sections were used as reference controls. The study records did not document the exact annatto solution concentration, preparation concentration, or the reagent concentrations and exposure times used for Masson's Trichrome, Van Gieson, and Ayoub–Shklar in the actual experiment; standard external protocols were therefore not substituted for the experimental conditions.

2.7 Histological Evaluation and Scoring

The stained sections were examined using a modified semi-quantitative framework comprising overall histological appearance, staining intensity, contrast, nuclear staining, cytoplasmic staining, specificity for the target tissue component, uniformity, clarity of tissue architecture, and diagnostic utility. Each parameter was assigned a score from 0 to 3, with higher scores indicating more favorable staining characteristics. Specificity referred to preferential staining of the intended tissue component and was distinguished from staining intensity. The sections were assessed in a blinded manner by oral pathologists; however, the study records did not specify the number of observers, the exact blinding procedure, or observer-level scores. Therefore, interobserver agreement could not be calculated retrospectively.

Table 1. Histopathological scoring criteria used to evaluate staining characteristics

Parameter	Score 0	Score 1	Score 2	Score 3
Overall Histological Appearance	Poor	Fair	Good	Excellent
Staining Intensity	Absent	Mild	Moderate	Strong
Contrast	Poor	Fair	Good	Excellent
Nuclear Staining	Absent	Poor	Moderate	Excellent
Cytoplasmic Staining	Absent	Poor	Moderate	Excellent
Specificity for Target Tissue Component*	Absent	Low	Moderate	High
Uniformity of Staining	Patchy	Uneven	Mostly uniform	Uniform
Clarity of Tissue Architecture	Poor	Fair	Good	Excellent
Diagnostic Utility	Not useful	Limited	Useful	Highly useful

** Specificity for the target tissue component was assessed according to the degree of preferential staining of the intended histological component.*

The nine scoring parameters were retained as individual 0–3 criteria. The available study records contain only aggregate percentage values and do not document the exact observer-level aggregation procedure or denominator used to generate each percentage. The reported percentages are therefore retained as descriptive values without reconstructing unrecorded raw scores or assigning statistical significance.

2.8 Statistical Analysis

No inferential statistical test was performed because the available dataset contained aggregate percentage scores without the underlying observer-level measurements, specimen-level replication, or a documented observer count. The percentages are therefore presented descriptively, and no statistical significance, superiority, or equivalence is claimed. A future study should prospectively define the number of specimens and observers and retain individual 0–3 scores to permit between-method testing and interobserver agreement analysis.

3. RESULTS

3.1 Optimization of Annatto Staining Duration

The staining duration was initially assessed by evaluating natural and commercial Bixa orellana (annatto) preparations at 5, 15, and 30 min. Based on the recorded visual assessment of overall staining quality, 5 min was selected for both preparations and used in the subsequent comparison. This optimization was preliminary and qualitative; numerical scoring data for the three time points were not available, and no inferential comparison was performed.

Table 2. Optimization of staining duration for natural and commercial *Bixa orellana* (annatto) preparations

Annatto Preparation	Duration Evaluated	Selected Duration
Natural *Bixa orellana* extract	5, 15, and 30 min	5 min
Commercial annatto preparation	5, 15, and 30 min	5 min

3.2 Characterization of the Iron Oxide Nanoparticle-incorporated Annatto Formulation

3.2.1 FTIR Analysis

FTIR analysis of the iron oxide nanoparticle-incorporated annatto formulation showed absorption bands at 3261.3, 2931.8, 1605, 1399.4, 1042.8, 885.24, 715.04, and 586.5 cm^{-1}. The broad band at 3261.3 cm^{-1} is compatible with O–H stretching, while the band at 2931.8 cm^{-1} is compatible with aliphatic C–H stretching. The bands near 1605 and 1399.4 cm^{-1} may represent overlapping contributions from aromatic/conjugated and oxygen-containing plant constituents, and the band at 1042.8 cm^{-1} is compatible with C–O/C–O–C vibrations. The lower-wavenumber bands were interpreted descriptively. The band at 586.5 cm^{-1} lies in a region where Fe–O lattice vibrations can occur; however, because annatto-only and FeONP-only spectra were unavailable, the FTIR data do not establish a specific nanoparticle–extract interaction (Silva et al. 2024).

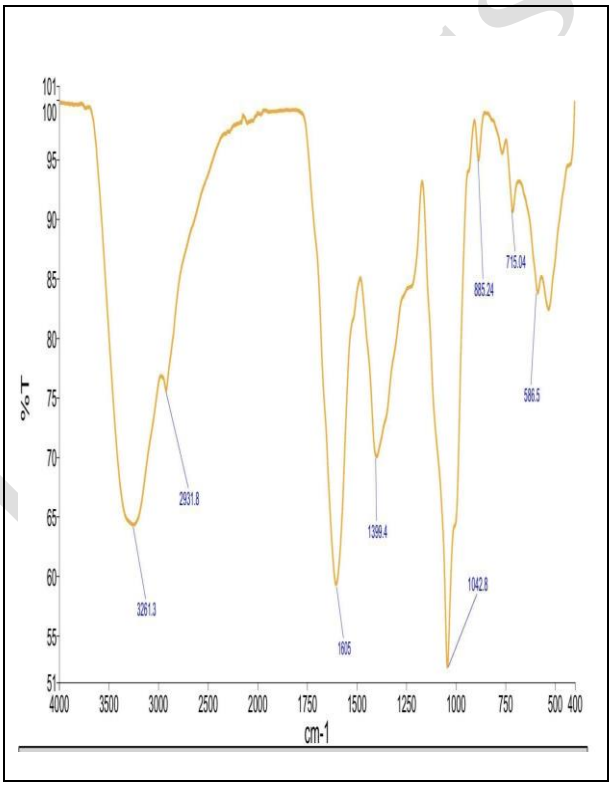


Fig. 2: FTIR spectrum of the iron oxide nanoparticle-incorporated *Bixa orellana* (annatto) formulation, showing absorption bands at 3261.3, 2931.8, 1605, 1399.4, 1042.8, 885.24, 715.04, and 586.5 cm^{-1}. The spectrum represents the combined formulation; an annatto-only comparator was not available.

3.2.2 XRD Analysis

XRD analysis of the iron oxide nanoparticle-incorporated annatto formulation showed 15 identifiable diffraction features at 16.933°, 21.436°, 23.689°, 28.302°, 29.390°, 38.422°, 39.353°, 40.360°, 42.028°, 43.152°, 44.676°, 47.464°, 48.545°, 65.088°, and 78.218°. The corresponding d-spacings ranged from 5.23203 to 1.22115 Å, and the recorded net intensities ranged from 93.4861 to 3300.30 counts. The reported XRD-derived crystallite-size estimates ranged from 17.4 to 69.6 nm. These values represent coherent diffracting domains rather than direct particle-size measurements. The original analysis also reported 46.4% crystalline and

Articles

53.6% amorphous fractions; however, the calculation method and software were not documented, so these values are retained only as formulation-level descriptive findings. No validated JCPDS/ICDD phase match was available; therefore, the iron oxide phase is not assigned conclusively.

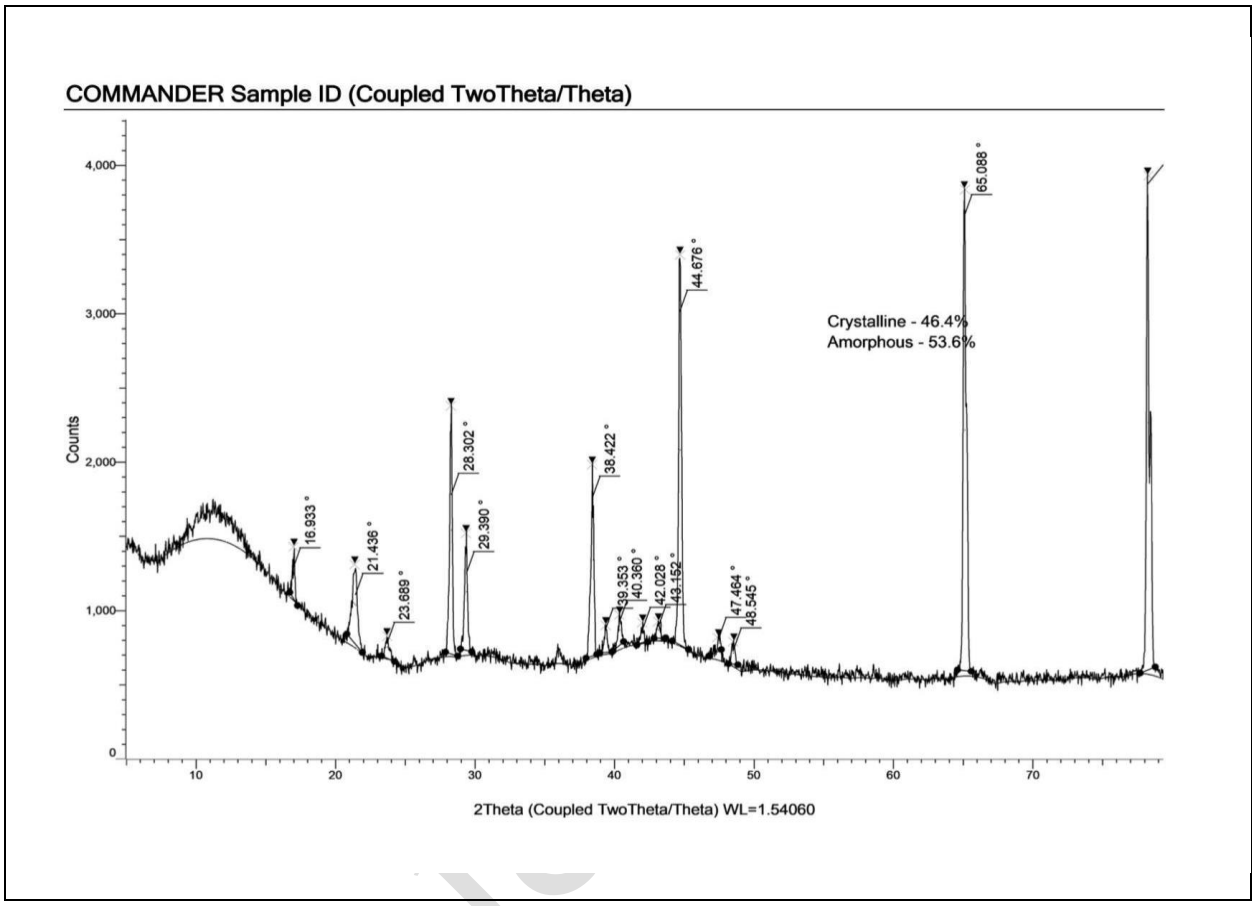


Fig. 3: XRD diffractogram of the iron oxide nanoparticle-incorporated *Bixa orellana* formulation. The recorded diffraction features are shown across the measured 2θ range; the original analysis reported 46.4% crystalline and 53.6% amorphous fractions. These are presented as formulation-level descriptive values and are not assigned exclusively to the iron oxide component.

3.3 Histopathological Staining Findings

Annatto preparations demonstrated variable staining distribution across the evaluated tissue components. In fibroma, commercial and natural annatto showed diffuse connective-tissue stromal staining, whereas the iron oxide nanoparticle-incorporated formulation also stained the stromal tissue. In OSMF, annatto preparations stained the connective-tissue stroma and overlying epithelium, while the nanoparticle-incorporated formulation showed visually distinct delineation of collagen fiber bundles. These observations describe visual distribution and intensity and are interpreted alongside the aggregate scoring data rather than as evidence of molecular specificity.

In keratinized tissue, commercial and natural annatto stained keratin pearls, with relatively greater peripheral coloration, while the nanoparticle-incorporated formulation showed prominent keratin staining. In odontogenic lesions, commercial and natural annatto stained connective tissue surrounding dental hard tissues, while ghost cells showed no appreciable staining. The nanoparticle-incorporated formulation stained odontogenic epithelium in ameloblastoma, but the intensity was similar to that of the surrounding stroma, limiting apparent specificity.

Annatto staining was also observed in blood vessels, adipose tissue, and ductal elements. The nanoparticle-incorporated formulation showed comparatively greater visual staining in some connective-tissue and ductal areas. Because the available analysis is descriptive, these observations are not interpreted as proof of increased staining specificity or diagnostic superiority.

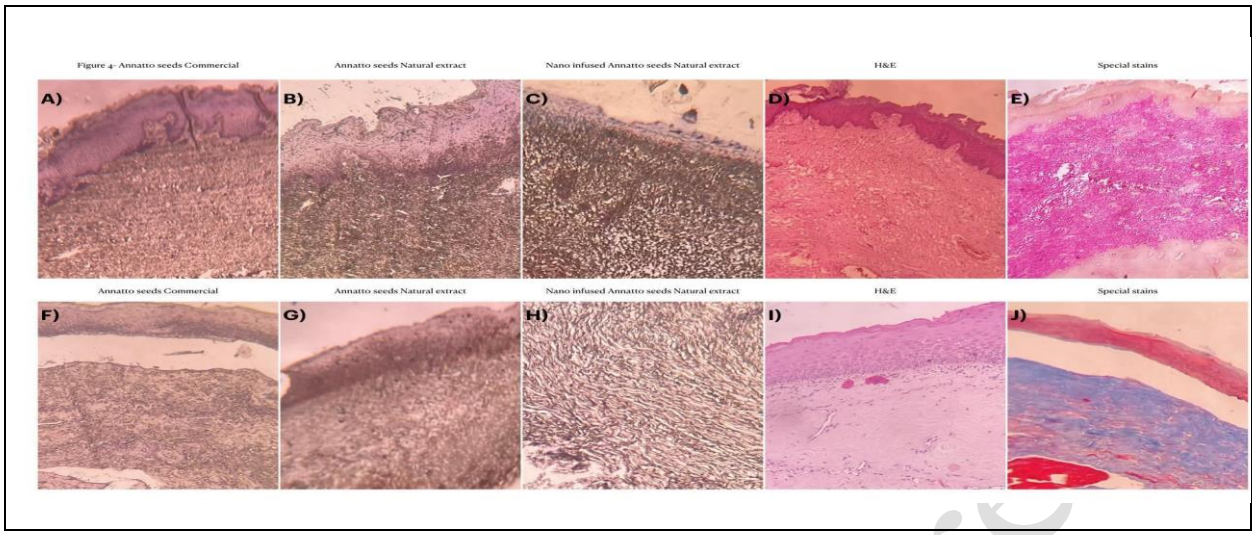


Fig. 4: Histochemical evaluation of annatto preparations in fibroma and oral submucous fibrosis. A: Commercial annatto-stained fibroma showing diffuse connective-tissue stromal staining; B: Natural annatto-stained fibroma showing comparatively greater staining intensity; C: Iron oxide nanoparticle-incorporated annatto formulation showing prominent stromal staining; D: H&E-stained fibroma; E: Corresponding conventional special-stained fibroma; F: Commercial annatto-stained OSMF showing diffuse stromal and lower epithelial staining; G: Natural annatto-stained OSMF showing similar distribution with greater intensity; H: Iron oxide nanoparticle-incorporated annatto formulation showing delineation of collagen fibre bundles; I: H&E-stained OSMF; J: Corresponding conventional special-stained OSM

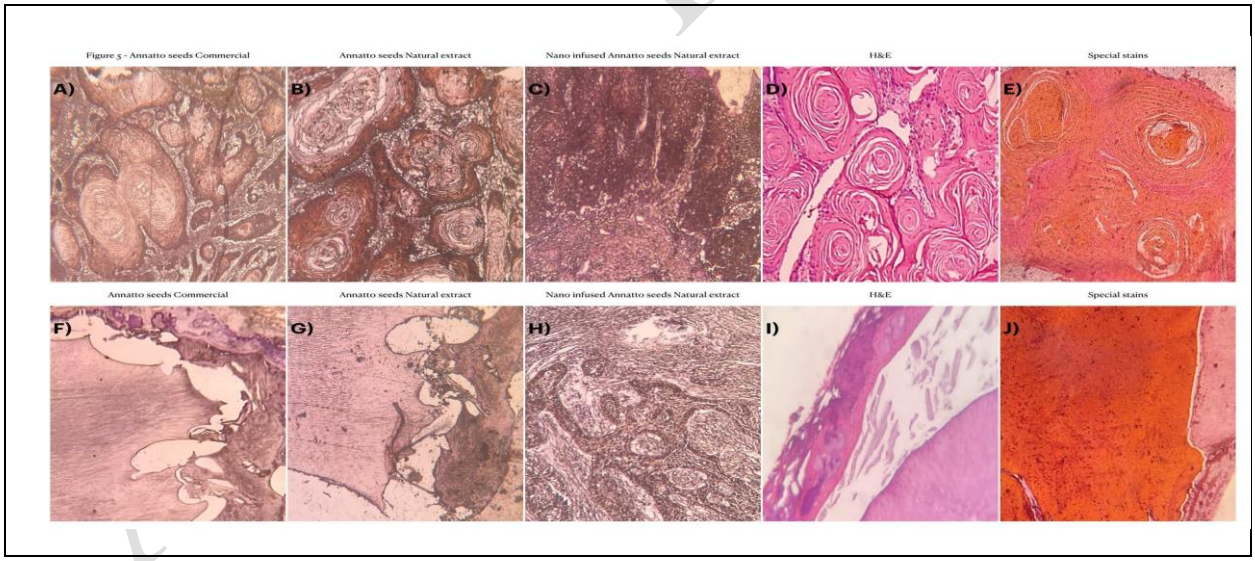


Fig. 5: Histochemical evaluation of annatto preparations in keratinized and odontogenic tissues. A: Commercial annatto-stained keratinized tissue showing keratin pearl staining with relatively greater peripheral intensity; B: Natural annatto-stained tissue showing similar keratin pearl staining; C: Iron oxide nanoparticle-incorporated annatto formulation showing prominent keratin staining; D: H&E-stained corresponding keratinized tissue; E: Corresponding conventional special-stained tissue; F: Commercial annatto-stained odontoma showing staining of connective tissue surrounding dental hard tissue, with no appreciable ghost-cell staining; G: Natural annatto-stained odontoma showing a similar distribution with absent ghost-cell staining; H: Iron oxide nanoparticle-incorporated annatto formulation in ameloblastoma showing odontogenic epithelial staining without clear separation from the surrounding stroma; I: H&E-stained corresponding odontogenic lesion; J: Corresponding conventional special-stained section

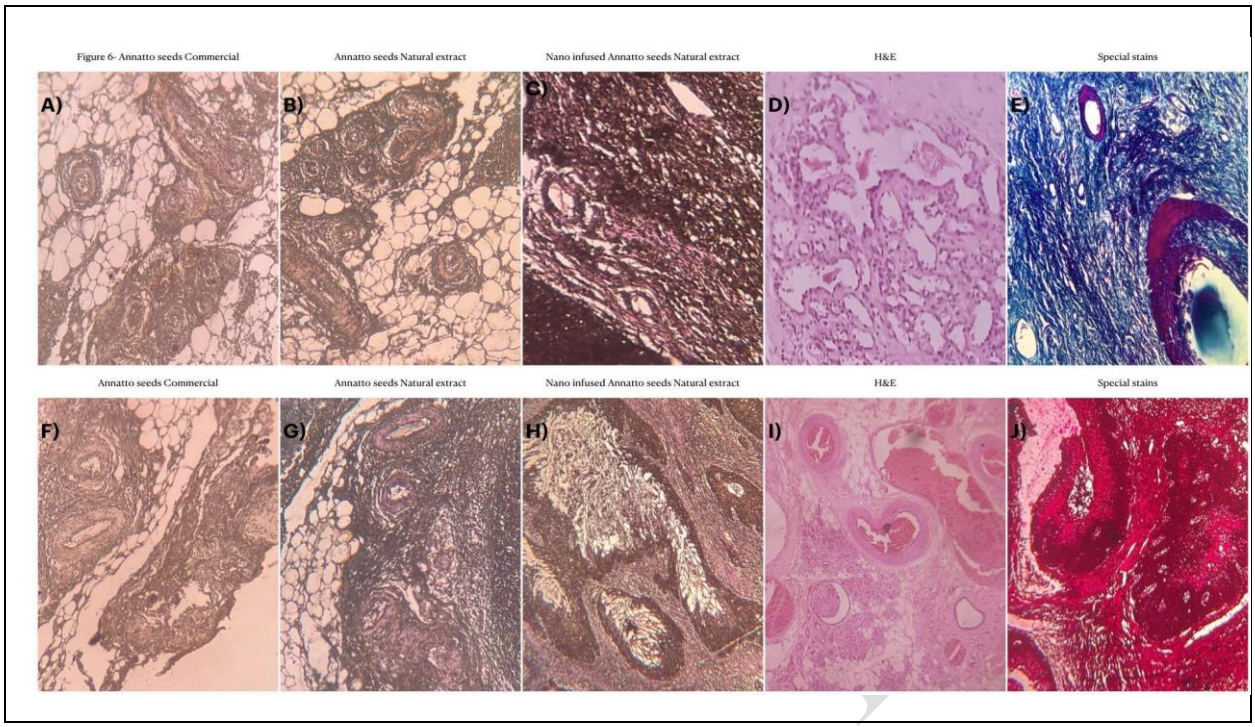


Fig. 6. Histochemical evaluation of annatto preparations in vascular, adipose, and ductal tissue components. A: Commercial annatto-stained section showing blood vessels, adipose tissue, and ductal elements; B: Natural annatto-stained section showing the corresponding tissue components; C: FeONP-incorporated annatto formulation showing comparatively increased staining in connective tissue, vessels, adipose tissue, and ductal elements; D: H&E-stained section; E: Corresponding conventional special-stained section; F: Commercial annatto-stained section showing vascular, adipose, and ductal components; G: Natural annatto-stained section showing the corresponding components; H: FeONP-incorporated annatto formulation showing comparatively increased connective-tissue and ductal staining; I: H&E-stained section; J: Corresponding conventional special-stained section

3.3.1 Histopathological Scoring

The stained sections were evaluated using the predefined 0–3 scoring system covering nine parameters. The percentage scores for the evaluated staining methods are presented in Table 3. Because observer-level data were unavailable, the reported values are descriptive aggregate scores. The lesion-wise values are internally consistent with the reported overall means, which represent the aggregate mean across the five tissue/lesion categories.

Table 3. Descriptive percentage scores for the evaluated staining methods; values are aggregate percentages from the original analysis and should not be interpreted as inferential comparisons

Tissue/ Lesion	Commercial Annatto	Natural Annatto	FeONP-incorporated Formulation	H&E	Conventional Special Stain
Fibroma	74.07%	77.77%	64.81%	81.48%	66.66% (Van Gieson)
OSMF	66.66%	44.44%	75.92%	88.88%	81.48% (Masson's Trichrome)
OSCC: Keratin pearls/ epithelial islands/ glandular epithelium	55.55%	62.96%	72.22%	85.18%	74.07% (Ayoub–Shklar)
Odontogenic tumors: Odontome, Ameloblastoma	71.42%	61.90%	74.07%	85.71%	85.71% (Ayoub–Shklar)
Blood vessels, ductal elements and adipose tissue	64.81%	72.22%	68.51%	82.40%	62.96% (Masson's Trichrome)
Overall mean score	66.5%	63.85%	71.10%	84.73%	74.17%

The overall mean percentage scores were 63.85% for natural annatto, 66.50% for commercial annatto, 71.10% for the iron oxide nanoparticle-incorporated formulation, 84.73% for H&E, and 74.17% for the corresponding conventional special stains. Among the annatto preparations, the nanoparticle-incorporated formulation had the highest descriptive overall score. Its lesion-wise scores were 64.81% in fibroma, 75.92% in OSMF, 72.22% in OSCC, 74.07% in odontogenic tumors, and 68.51% in blood vessels, ductal elements, and adipose tissue. These values do not support statistical significance, superiority, or equivalence claims. The 71.10% score for the nanoparticle-incorporated formulation was numerically below the conventional special-stain score of 74.17% and H&E score of 84.73%.

4. DISCUSSION

Conventional histochemical stains remain important reference methods because their tissue affinities and diagnostic applications are established. In this pilot study, annatto produced visible staining across several oral tissue components, while the nanoparticle-incorporated formulation produced the highest descriptive score among the annatto preparations. The numerical score remained below both conventional special stains and H&E, and the absence of inferential analysis prevents conclusions regarding statistical differences or equivalence.

The descriptive scores indicate that the nanoparticle-incorporated formulation can provide useful visual contrast in selected tissues, but its performance was not equivalent to the reference methods on the available aggregate data. In OSMF, the formulation had the highest annatto-group score and visually delineated collagen fiber bundles. These observations support further investigation but do not establish diagnostic specificity or replacement of established collagen stains.

The most evident staining affinity involved collagen-rich connective tissue. The OSMF findings were consistent with the expected utility of Masson's Trichrome and Van Gieson for collagen-rich tissue (Benard et al. 2017; Van de Vlekkert et al. 2020). However, collagen was not quantified biochemically, and the present staining observations cannot establish molecular specificity. The possibility that iron oxide nanoparticles altered pigment dispersion remains a hypothesis because dispersion, particle–pigment interaction, and tissue binding were not directly measured.

In keratinized tissue, annatto-stained keratin pearls and the nanoparticle-incorporated formulation showed prominent coloration. Ayoub–Shklar is an established keratin stain (Dineja et al. 2024); therefore, the present findings indicate pigment affinity for keratinized structures rather than diagnostic specificity. Staining intensity should not be equated with selective identification of the target component.

In odontogenic lesions, staining was mainly observed in connective tissue surrounding dental hard tissues. The nanoparticle-incorporated formulation also stained odontogenic epithelium in ameloblastoma, but the intensity was not clearly separated from the surrounding stroma. The absence of ghost-cell staining was observed in the available odontoma specimen and should not be generalized beyond the evaluated material.

Staining of vascular, ductal, and adipose components indicates broad tissue affinity rather than high specificity. Such distribution may provide visual contrast, but it may also reduce diagnostic discrimination when the target structure and surrounding tissue show similar coloration.

FTIR and XRD provided preliminary characterization of the combined annatto–iron oxide formulation. The FTIR bands were compatible with functional groups from plant-derived constituents, with the low-wavenumber band occurring in a region where Fe–O vibrations may occur; however, the absence of annatto-only and FeONP-only spectra prevents attribution of formulation-specific changes. XRD showed multiple diffraction features and an amorphous background. The reported 46.4% crystalline and 53.6% amorphous fractions require cautious interpretation because the calculation method and software were not documented. Similarly, the reported 17.4–69.6 nm values are crystallite-size estimates, not direct particle sizes, and the iron oxide phase was not conclusively identified.

The principal limitations were incomplete specimen and observer documentation, missing formulation and extraction parameters, unavailable observer-level scores, and incomplete instrumental operating details. Direct particle-size and colloidal-stability measurements were not available, and the XRD phase assignment and crystalline/amorphous calculation could not be independently verified. The study also did not quantitatively assess reagent use, waste, toxicity, biodegradability, life-cycle impact, or cost. The findings should therefore be regarded as preliminary evidence of staining affinity. Future studies should prospectively document specimen numbers, observer-level scores, standardized staining protocols, complete formulation parameters, direct nanomaterial characterization, and objective image-based or inferential evaluation.

5. CONCLUSION

The present pilot study demonstrated preliminary staining affinity of Bixa orellana (annatto) in selected oral tissues, particularly collagen-rich

Article In Press

connective tissue, with additional staining of keratinized, vascular, ductal, and adipose components. The iron oxide nanoparticle-incorporated formulation showed the highest descriptive score among the annatto preparations; however, the available aggregate data do not establish diagnostic specificity, equivalence to conventional special stains, or suitability as a diagnostic replacement. The findings provide a preliminary basis for further investigation of annatto-based staining components, while their environmental relevance remains to be established because reagent use, waste generation, toxicity, biodegradability, life-cycle impact, and cost were not quantitatively assessed. Future studies should incorporate standardized staining protocols, complete specimen- and observer-level data, direct nanomaterial characterization, and quantitative environmental assessment to determine the reproducibility, performance, and environmental implications of such formulations.

ACKNOWLEDGEMENT

The authors express their sincere gratitude to Saveetha Dental College and Hospitals, Saveetha Institute of Medical and Technical Sciences, Chennai, for providing the necessary facilities and support for conducting this study.

FUNDING

This research received no specific grant from any funding agency in the public, commercial, or not-for-profit sectors.

CONFLICTS OF INTEREST

The authors declare that there is no conflict of interest.

COPYRIGHT

This article is an open-access article distributed under the terms and conditions of the Creative Commons Attribution (CC BY) license (http://creativecommons.org/licenses/by/4.0/).



REFERENCES

Aiswarya, A. M., Patel, B., Tiwari, H., Doria, G., Mehta, R. and Asnani, P., Alternatives to eosin in histopathological assessments: a comparison of organic stains, J. Oral Maxillofac. Pathol., 29(4), 563-570 (2025). https://doi.org/10.4103/jomfp.jomfp_128_25

Balabadra, K.M., Panneer Selvam, S., Ramadoss, R. and Sundar, S., Hydroxyapatite synthesis and characterization from marine sources: A comparative study, J. Oral Biol. Craniofac. Res., 14(6), 706-711 (2024). https://doi.org/10.1016/j.jobcr.2024.09.009

Benard, S., Solomon, O., Fowotade, A. A., Okoye, J., Kayode, B. and Abiola, O., Hibiscus-Van Gieson stain for collagen fibres, Afr. J. Cell Pathol., 9(12), 1-4 (2017).

Devendrababu, Y., Vikram, V. and Tamilarasi, A., Safer and sustainable alternatives to xylene in histopathology: a comprehensive review, J. Appl. Toxicol., 46(3), 775-792(2026). https://doi.org/10.1002/jat.70029

Dilmurodov, D. D., Maxmedov, S. V., Yuldoshov, J. D., Shavkatov, O. T. and Ishandjanova, S. X., The use of nanotechnologies in histological research, Galaxy Int. Interdiscip. Res. J., 13(6), 2347-2351 (2025).

Dineja, R., Prasad, H., Chinthu, K. S. and Rajmohan, M., Ayoub-Shklar as a special stain for keratin: a histopathological study, J. Microsc. Ultrastruct., 12(3), 109-113 (2024). https://doi.org/10.4103/jmau.jmau_34_23

Gurina, T. S. and Simms, L., Histology, Staining, Nat. Library Med., (2023). https://www.ncbi.nlm.nih.gov/books/NBK557663/

Husain, O., Wargasetia, T. L., Gunadi, J. W. and Hamdan, A. R., Quantitative Histomorphometric Analysis of Collagen Bundles in Masson's Trichrome Stained Rat (Rattus norvegicus) Skin: A Methodological Study, Hea. Sci. Rep., 9(3), e71998 (2026). https://doi.org/10.1002/hsr2.71998

Kattookaran, C.V., Govindasamy, R., Panneer Selvam, S. and Viswanathan, D., Biosynthesis of Ag-doped MgO-ZnO nanocomposite with Cassia alata plant leaves extract and assessment of their biological applications, Next Mater., 8, 100820 (2025). https://doi.org/10.1016/j.nxmate.2025.100820

Krampah, C., Nyanzu, F., Quaye, A., Adu, P., Asiamah, E. A., Aboagye, B. and Simpong, D. L., Crude extracts from Allium cepa skin and Sorghum bicolor seed can provide as non-toxic and eco-friendly cytoplasmic stains, *Pract. Lab Med.*, 26, e00239 (2021). https://doi.org/10.1016/j.plabm.2021.e00239

National Institute for Occupational Safety and Health (NIOSH), Xylene, Centers for Disease Control and Prevention, last reviewed 2019. https://www.cdc.gov/niosh/topics/xylene/ (2019).

Rabbi, M. A., Akter, M. B., Chaki, B. M., Latif, M. A., Al-Amin, M., Rasel, M. Z. U., Sharmin, S., Abdurrahim, M., Rubel, M. H. K. and Habib, M. R., Preparation of stable Fe2O3/Ag nanocomposite particles with catalytic, antioxidant and antibacterial properties, New J. Chem., 48(12), 5278-5288 (2024). https://doi.org/10.1039/D3NJ05885A

Article in Press

Shahid-ul-Islam, Rather, L. J. and Mohammad, F., Phytochemistry, biological activities and potential of annatto in natural colorant production for industrial applications: a review, J. Adv. Res., 7(3), 499-514 (2016). https://doi.org/10.1016/j.jare.2015.11.002

Sikaria, S., et al., Membrana preformativa: Unveiling the unexplored facets of dental development, J. Oral Biol. Craniofac. Res., 15(1), 84-87 (2025). https://doi.org/10.1016/j.jobcr.2024.12.010

Silva, V. R. P., Martins, N. O., Santos, C. R., Damas, E. B. O., Araujo, P. L., Silva, G. O., Joanitti, G. A. and Carneiro, M. L. B., Annatto (*Bixa orellana*)-Based Nanostructures for Biomedical Applications—A Systematic Review, *Pharma.*, 16(10), 1275 (2024). https://doi.org/10.3390/pharmaceutics16101275

Sureshbabu, S., Arthanari, A. and Shanmugam, R., Green synthesis of silver nanoparticles using Althaea officinalis and Pterocarpus santalinus formulation and its anti-inflammatory and antimicrobial activity against oral wound pathogen, *J. Environ. Nanotechnol.*, 15(2), 640-648 (2026). https://doi.org/10.13074/jent.2026.06.2622257

Van de Vlekkert, D., Machado, E. and d'Azzo, A., Analysis of generalized fibrosis in mouse tissue sections with Masson's trichrome staining, *Bio Protocol*, 10(10), e3629(2020). https://doi.org/10.21769/BioProtoc.3629

Yameen, M., Adeel, S., Salman, M., Haji, A., Asghar, F., Mia, R. and Imran, M., Sustainable appraisal of lipstick tree seeds (*Bixa orellana*)-based bixin natural orange colorant for green mordanted silk fabrics and wool yarns, *Sci. Prog.*, 107(2), 368504241242282 (2024). https://doi.org/10.1177/00368504241242282

Article in Press